CEOCOR

MALMO Sweden Hilton Hotel
1st June – 3rd June, 2005

SECTOR A - PAPER N. 2

Investigating AC and DC stray current corrosion

FR

Étude de la corrosion par courants vagabonds CA et CC

D

Korrosionsuntersuchungen bei Gleich - und Wechselstrom Streuströmen

A report from the Danish activities

L.V. Nielsen
Metri\Corr ApS, Glerupvej 20, DK-2610 Roedovre, Denmark

B. Baumgarten
HNG I/S – Greater Copenhagen Natural Gas
Gladsaxe Ringvej 11, DK-2860 Soeborg, Denmark

P. Cohn,
Gastra A/S, Bregnerødvej 133D, 3460 Birkerød, Denmark

Abstract
Combined and individual effects of AC and DC stray currents on corrosion of buried pipelines are studied in a research program jointly within the Danish natural gas transmission/distribution companies.

Studies have given evidence for the alkalisation mechanism, and it has been shown both in field and in laboratory soil box experiments that AC corrosion stops at low CP dosage and accelerates at high dosage of CP. Cathodic DC density controls the spread resistance at a coating defect. In turn, the spread resistance controls the level of AC density – at given AC voltage. High level of DC density (>3-5 A/m2) in combination with (even rather low >5-10 V) AC voltage gives AC corrosion.
DC density and spread resistance are primary factors in judgment of AC corrosion likelihood.
Combined effect of DC stray currents and AC may cause corrosion both in terms of the alkalisation mechanism that characterises “traditional” AC corrosion, and in terms of the anodic DC peaks occurring in DC stray interference.

Résumé
En conséquence du mécanisme d'alcalisation lié à la corrosion due au CA, il est recommandé de maintenir le potentiel à un niveau faible afin de ménager l'état de la PC et d'éviter un excès de courant de PC. Une question particulièrement intéressante dans ce contexte est l'impact de cette précaution sur l'efficacité de la protection contre les courants vagabonds CC.

Cet article inclura les résultats de 2 différentes séries d'expériences avec soil box.

Une série dans laquelle une matrice des conditions CA/CC a été examinée pour connaître les circonstances provoquant une corrosion CA. Une autre dans laquelle une PC faible a été combinée à de fréquentes pointes de courant anodique afin d'analyser les risques de corrosion par courants vagabonds CC.

Ces observations sont débattues en tenant compte de divers paramètres pratiques pertinents.

Introduction

Combined effects of AC and DC stray currents on corrosion of buried pipelines are studied in a research program supported by the Danish Gas Technology Centre (DGC), which is jointly owned by the Danish natural gas transmission/distribution companies.
A report on some of the activities was given at CeoCor 2004.[1] One particular conclusion was concerned with the alkalisation mechanism of AC induced corrosion. In brief, this mechanisms proceeds when OH^- produced by cathodic protection current accumulates in the near surroundings of the coating defect (figure 1).[1-5] The combined action of potential vibration caused by the AC and adequately high pH induces corrosion attacks. Potential vibration in between the immunity and passivity region of the Pourbaix diagram (figure 2) may cause corrosion due to different time constants associated with iron dissolution (fast) and subsequent formation of passive film (slower). At very alkaline pH (14) the formation of dissolved $HFeO_2^-$ may stabilize corrosion at a very high penetration rate.

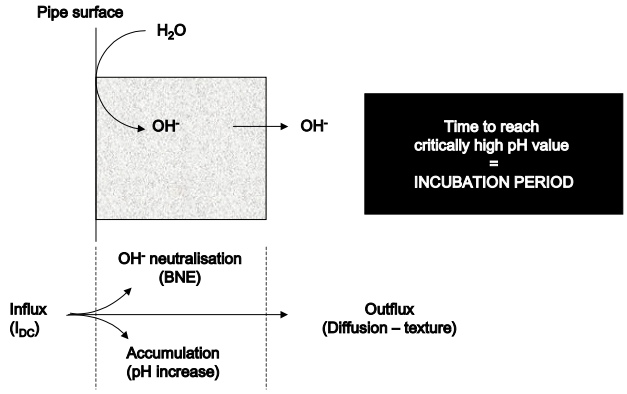

Figure 1. Mass balance schematics for OH- ions produced by CP at a coating defect.

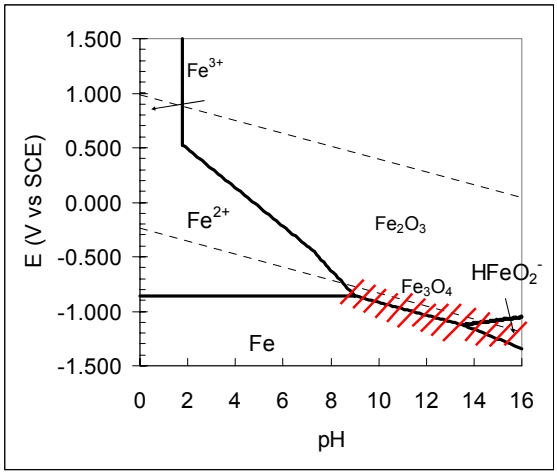

Figure 2. Pourbaix diagram showing unsafe region with respect to AC corrosion.

This present paper gives further evidence for the alkalisation mechanism by presenting results of both laboratory soil box experiments and field experience. Additionally, the combined effect of AC and DC stray current is illustrated based on initial results from a field investigation.

Experimental set-ups

The experimental procedures are practically the same for laboratory and field applications. A coupon is placed in the environment of interest to simulate a coating fault. In the laboratory soil box environment, the coupon is connected to a rectifier/transformer system, which, via a large inert counter electrode and a reference produces the desired AC/DC pattern on the coupon (figure 3 – left). In the field, the coupon is coupled to the pipe in the usual way. (figure 3 – right). The data logger assembly collects AC voltage, AC current, spread resistance (leakage

resistance) ON-potential and DC current. Usually electrical resistance coupons with standard element 2x20 mm = 0.4 cm^2 (or 3x33 mm = 1cm^2) size to simulate a small coating defect are employed. In this case, the corrosion of the coupon is logged on the data logger as well. Functionality of the instrumentation has been described elsewhere.[6]

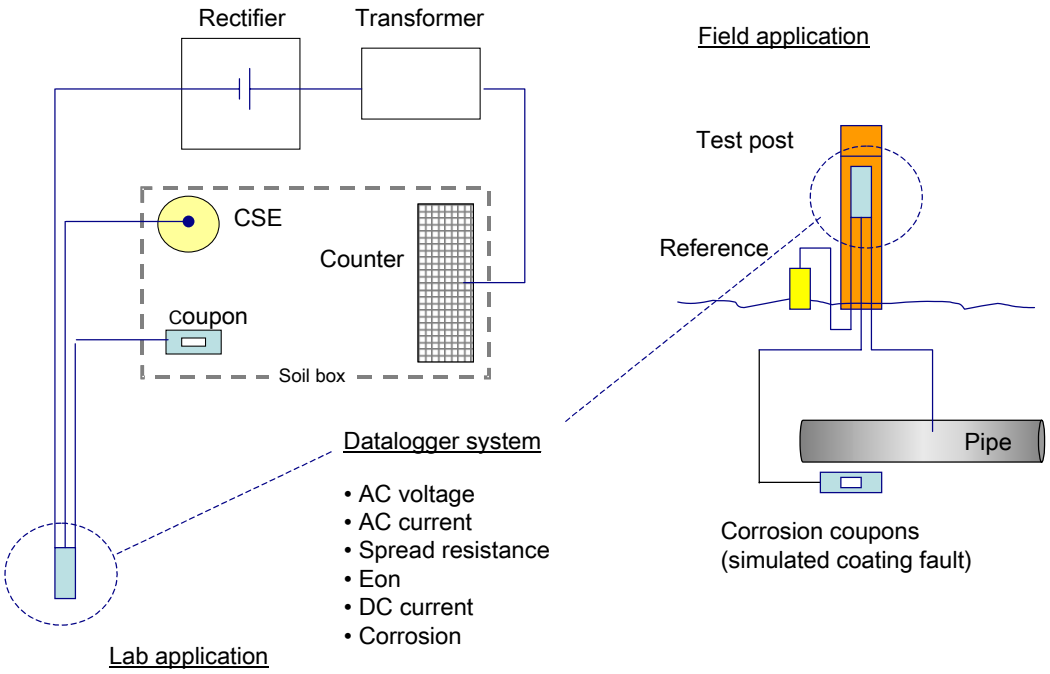

Figure 3. Experimental set-ups used in lab and in field.

Results and discussions

Laboratory soil box experiment – inert quartz sand + 0.01M NaCl solution.

A soil box experiment was set-up with a constant 15V AC voltage. The parameters were followed for some 60 days throughout which only the DC potential was adjusted*.

Figure 4 shows the corrosion rate throughout time, and as observed no corrosion occurs for the first 28 days. In this incubation period, the ON-potential was changed rather un-motivated from moderate (-1250 mV CSE) via low (-850) to the severe (-2200) which was kept until corrosion sets on. After 10 days with high CP, the corrosion increases but finds some steady state condition for some days at a low rate (10 micron/yr). After 37 days, the corrosion starts increasing and after 48 days, the corrosion rate exceeded 120 micron/yr. For the purpose of studying the particular effect of the DC potential, the CP-ON was decreased to – 850 (still 15 V AC), and the corrosion decayed. Subsequent alternations with a few days interval in DC potential between -850 and -2250 mV was made in order to study the reaction. As observed

* The results from this particular experiment (figs 4-7) were presented in the CeoCor 2004 paper (ref 1) but included here to take up the track.

from figure 4, the corrosion can be entirely controlled by decreasing CP – high CP gives corrosion – low CP eliminates corrosion.

The AC current density appears from figure 5. A steady increase in AC current density occurs after heavy CP is applied (around day 16), indicating a steady decrease in spread resistance. The development in spread resistance calculated by the fraction Uac/Iac is observed in figure 6. The spread resistance so calculated seems to decrease as the coupon-close environment alkalises. The DC OFF potential has been calculated as the ON-potential minus the Idc x Rs drop and shown in figure 7. As observed, the severe CP ON-condition (-2250 mV CSE) corresponds between -1100 and -1300 mV CSE (off) depending on the actual magnitude of the IR drop.

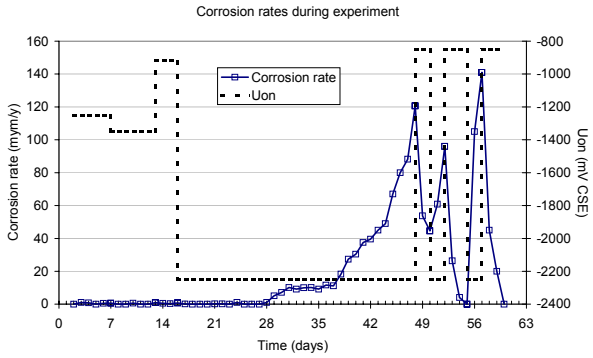

Figure 4. DC ON-potential and corrosion rate throughout time in the NaCl soil box experiment.

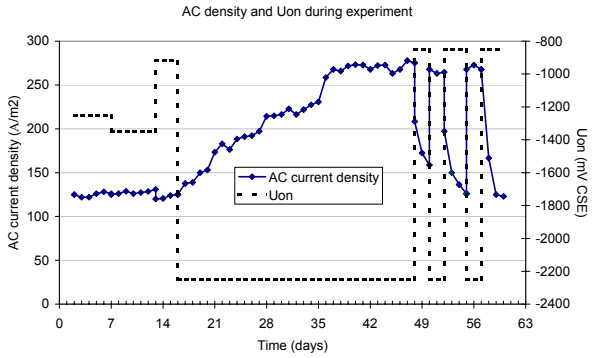

Figure 5. DC ON-potential and AC current density throughout time in the NaCl soil box experiment.

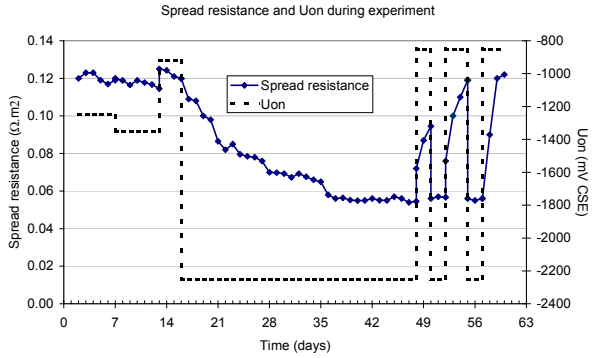

Figure 6. DC ON-potential and spread resistance throughout time in the NaCl soil box experiment.

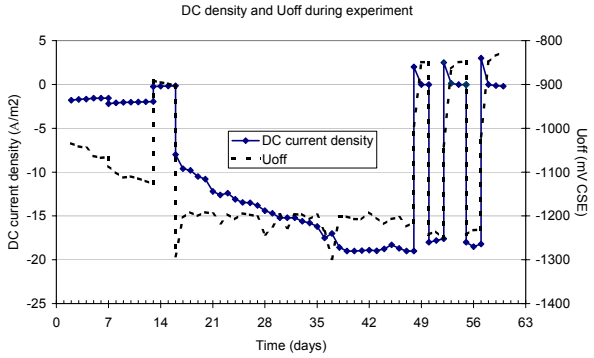

Figure 7. DC current density and IR compensated potential throughout time in the NaCl soil box experiment.

Figure 8 shows the correlation between DC current density (note: negative value is cathodic) and the AC current density at the coupon. It appears that for DC values above a certain value (in this case above ≈ 8 A/m2), a linear correlation between the DC density and the AC density exists. This may be explained by the influence of DC

on the spread resistance (figure 9). For DC densities above a certain value (≈ 8 A/m2), a linear correlation between DC and (inverse) spread resistance seems to be apparent. The higher the DC density, the lower the spread resistance, reflecting that the alkalinity production caused by DC entirely dominates the chemistry in vicinity of the coating defect. Since - at constant AC voltage - the AC density is determined by the (inverse) spread resistance, the correlation between DC density and AC density appears.

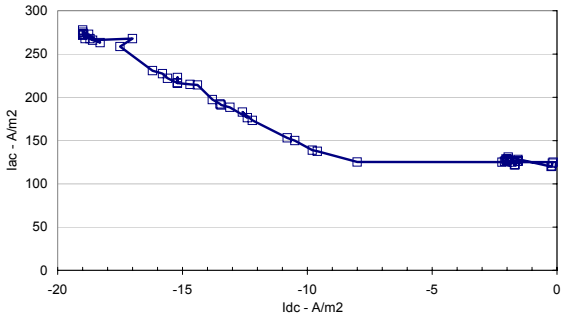

Figure 8. Correlation between AC and DC – NaCl soil box.

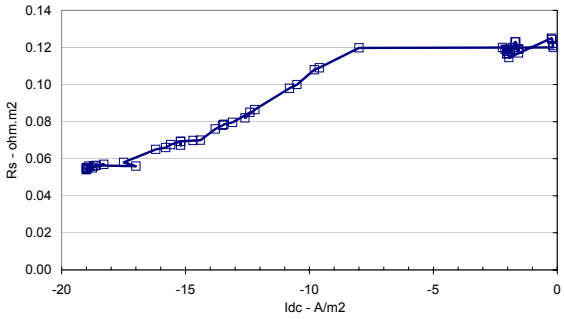

Figure 9. Correlation between DC and spread resistance – NaCl soil box.

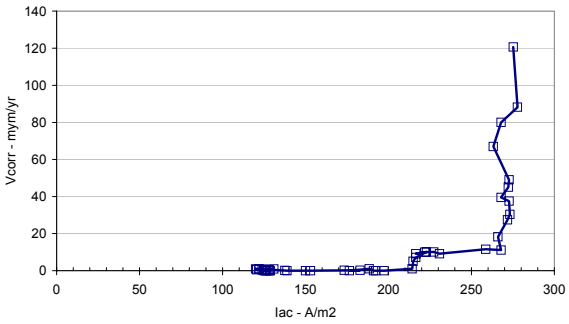

Figure 10. Correlation between AC and corrosion rate – NaCl soil box.

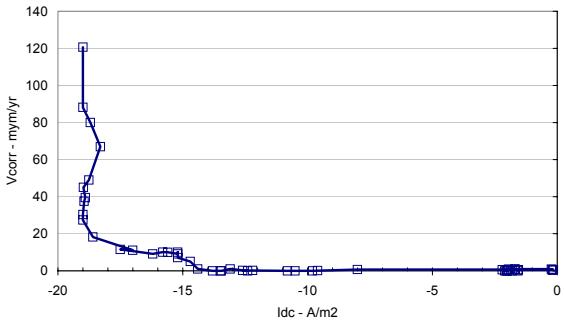

Figure 11. Correlation between DC and corrosion rate – NaCl soil box

Figure 10 shows the corrosion rate as a function of the AC density found in this environment. Although the AC density is often used as one way to judge AC corrosion likelihood[7], the interconnection between DC density, spread resistance, and AC density means that the DC density parameter should be equally important in judgements of the AC corrosion likelihood – figure 11.

Laboratory soil box experiment – inert quartz sand + 0.01M NaOH solution.

In order to reduce incubation period, a series of experiments has been performed in the inert quartz sand box with 0.01 M NaOH instead of NaCl. The pore water pH was then initially 12. In all experiments the AC voltage was adjusted to 15 V. 6 experiments were run over 2-3 weeks each and the electrical parameters and corrosion rate were recorded. The experiments differed by the applied DC ON potential (-850, -950, -1100, -1200, -1250, and –1300 mV CSE respectively).

Figures 12-17 show some results from these studies. All data from the six experiments have been merged into the graphs. In figure 12, the correlation between AC and DC density is illustrated. Apart from the results from the –850 mV experiment, the results are very consistent with figure 8 (AC level can be shown to correlate with DC level). Again, from figure 13, it is indicated that the spread resistance is entirely controlled by the DC density. Figures 14 and 15 show the corrosion rate as a function of the resulting AC density (figure 14) and DC density (figure 15). Both graphs show nice correlations.
Figure 16 is illustrating the dependency of the corrosion rate on AC voltage, which is practically absent. Figure 17 shows the dependency of the corrosion rate on the DC potential and the behaviour simply confirms that increased CP dosage increases the AC corrosion tendency.

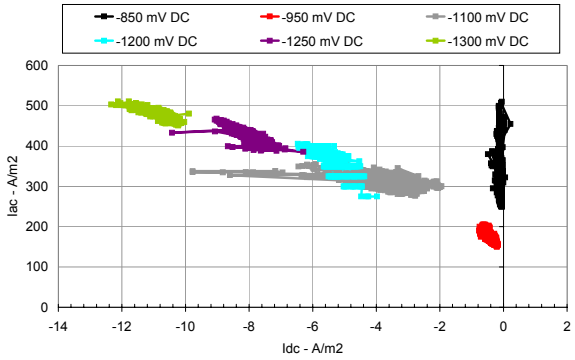

Figure 12. Correlation between AC and DC – NaOH soil box.

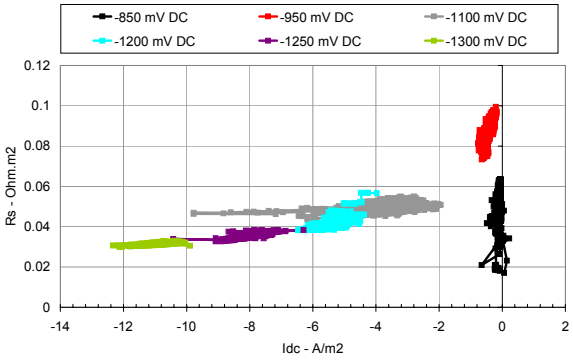

Figure 13. Correlation between DC and spread resistance – NaOH soil box.

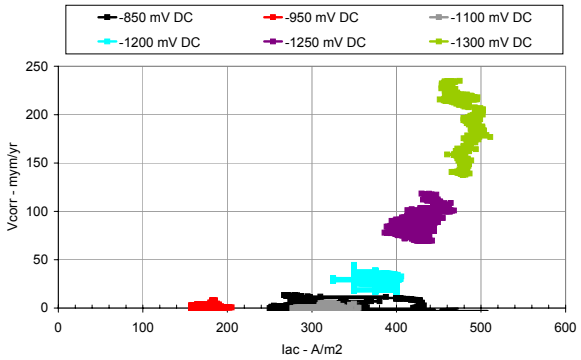

Figure 14. Correlation between AC and corrosion rate – NaOH soil box.

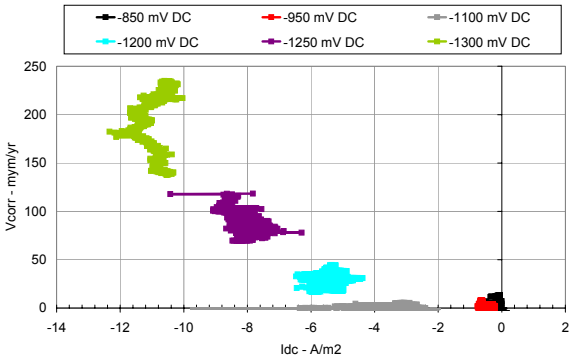

Figure 15. Correlation between DC and corrosion rate – NaOH soil box

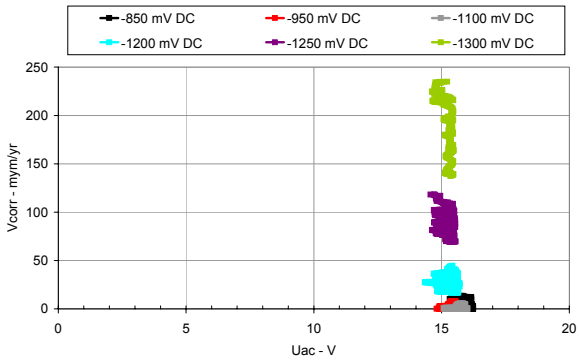

Figure 16. Correlation between Uac and corrosion rate – NaOH soil box.

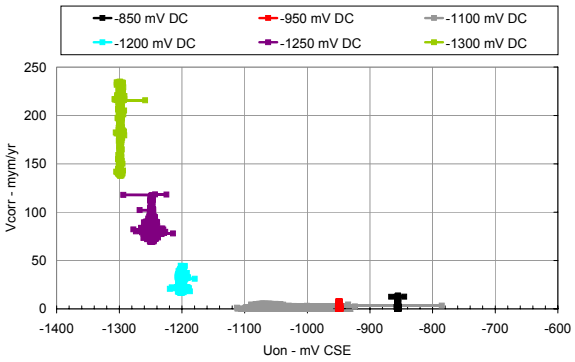

Figure 17. Correlation between Uon and corrosion rate – NaOH soil box

On-site measurements MR station – AC corrosion – alkalisation mechanism

Figures 18-23 show results obtained on ER coupons buried in a clayish soil at an MR station owned by HNG. Initially, both the AC voltage and the DC voltage were artificially produced by a rectifier/transformer system established at the MR station for this particular purpose. Several coupons have been tested all leading to the same conclusion as illustrated in the following concerning one such coupon.

Figure 18 shows the corrosion rate throughout time on the coupon. A build-up leading to a distinct peak (3 mm/yr, October 18th) is observed. Apart from one week where the adjusted AC voltage was 4 V, the coupon was maintained at 10 V during the whole build-up period. The DC ON –potential in this period was –1500 mV CSE (figure 20). Based on an IRs drop calculation, this potential corresponds to around –1100 mV CSE in the OFF condition.

At the exact time where the peak occurs the DC ON-potential is moderated to –1150 mV CSE (some –950 OFF). This causes an immediate decrease in corrosion rate (figure 18) however, without stopping corrosion entirely. November 9th when the AC voltage is decreased to 5 V (figure 19), the corrosion stops completely (figure 18). December 8th, the coupon was connected directly to the pipeline. This causes the AC voltage to alternate in between 0 and 10 V (figure 19) and the DC ON-potential to alternate between –1200 and –1300 mV CSE. From figure 18 is observed that these conditions are leading to corrosion yet again.

Figure 22 shows the very distinct peak in DC density (12 A/m2 at highest). Figure 23 shows the spread resistance as a function of the DC density – giving another proof of the large influence of the DC density on the spread resistance. In turn, the change in spread resistance gives changes in the AC density (figure 21) even though the AC voltage doesn't change. In conclusion, the same pattern as found in the controlled soil box experiments.

Figure 24 shows a nice correlation between corrosion rate and AC density, whereas figure 25 shows similarly a nice correlation between corrosion rate and DC density.

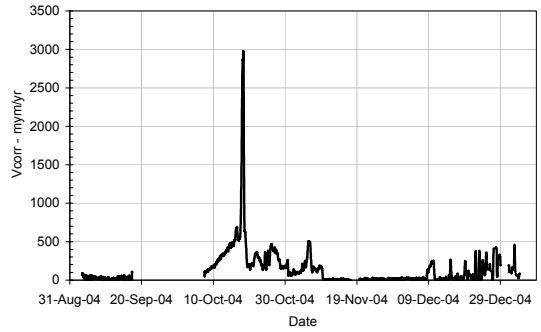

Figure 18. MR station – corrosion rate throughout time.

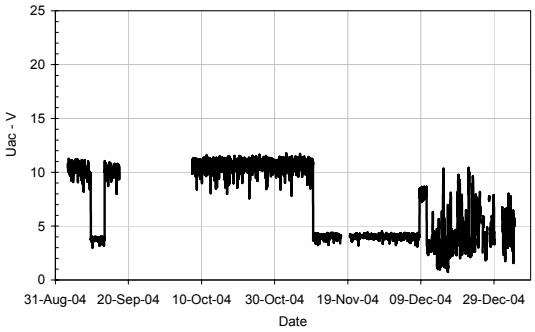

Figure 19. MR station – AC voltage throughout time.

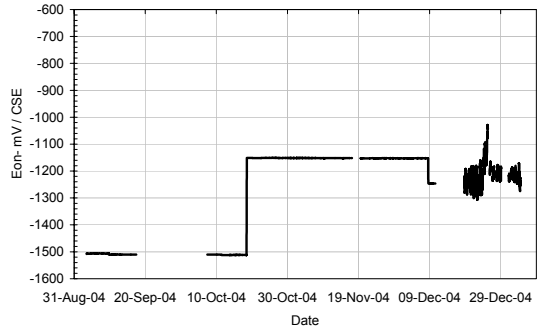

Figure 20. MR station – ON-potential throughout time.

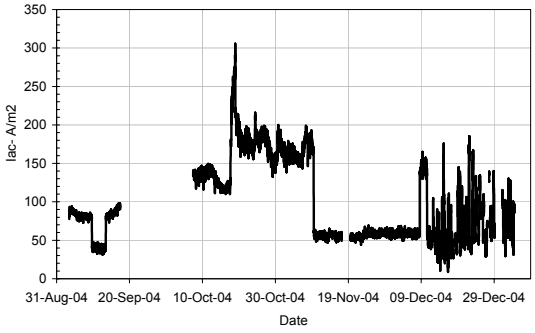

Figure 21. MR station – AC current throughout time.

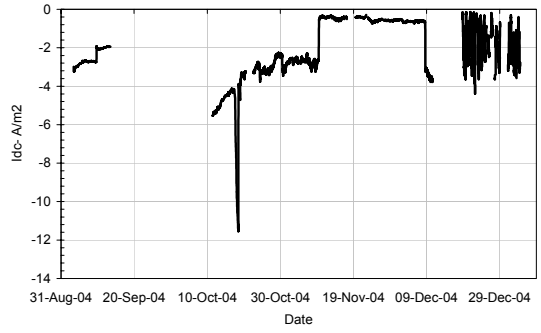

Figure 22. MR station – DC current throughout time.

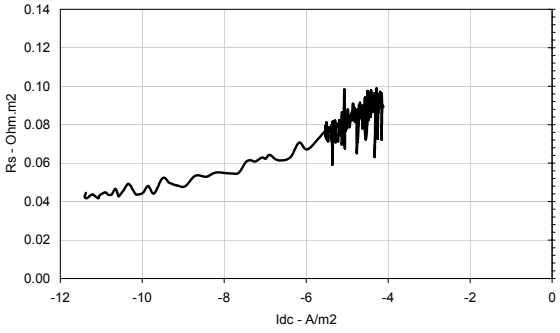

Figure 23. MR station - correlation between spread resistance and DC current.

.

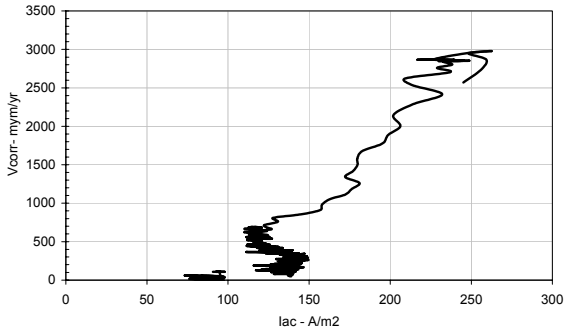

Figure 24. MR station - correlation between corrosion rate and AC current.

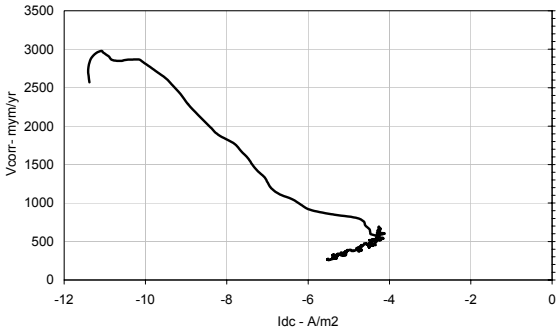

Figure 25. MR station - correlation between corrosion rate and DC current.

On-site measurements Railway station post – AC corrosion – DC stray current effect.

The last case described here is illustrated in figures 26-28. Coupons have been installed in a measuring post close to a railway station right next to the traction system and connected to the pipeline. The DC logger system was programmed to take readings every 5 seconds for a twenty minutes period. Such period was repeated 5 times a day; at 2-o'clock at night, at 7 o'clock in the morning (rush-hour and lots of trains) at 11 o'clock, at 15:00 and at 19:00. A typical pattern is shown in figure 26. Very little DC stray current at night (an un-disturbed and steady signal for both ON-potential and DC density), whereas the ON-potential changes within a 500-600 mV interval and accordingly the DC density in between zero and several A/m^2 during daytime.
The corrosion rate shown over a one-week period is illustrated in figure 27 along with the AC voltage. The peaks in those values both fall at night, but there seems to be some 4-5 hours between the corrosion rate peak and the AC voltage peak.

Figure 28 shows the DC pattern throughout the same week. One recognises the calm and steady conditions at night and the disturbed pattern throughout daytime. Anodic current peaks are frequent, but also very high cathodic DC currents are detected – as high as 8 A/m2. In combination with the AC voltage pattern typically exceeding 20V in peaks, there seems to be both concern for the corrosion caused by the anodic DC peaks, as well corrosion resulting from a combined effect of high cathodic DC current (producing alkalinity) and the AC voltage peaks.

This mixed AC/DC corrosion scenario is under further study in the Danish efforts.

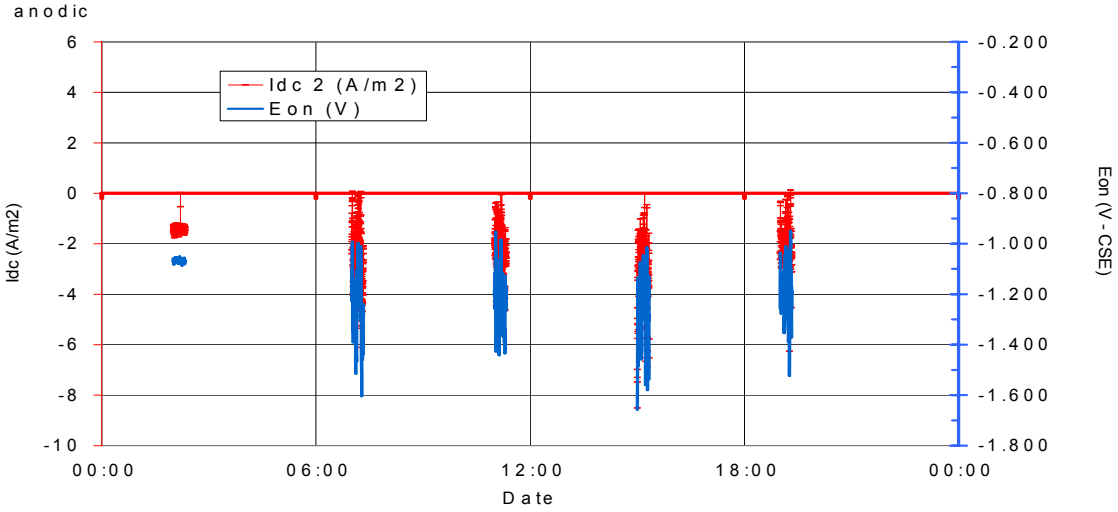

Figure 26. Railway station post– DC stray effect throughout the day.

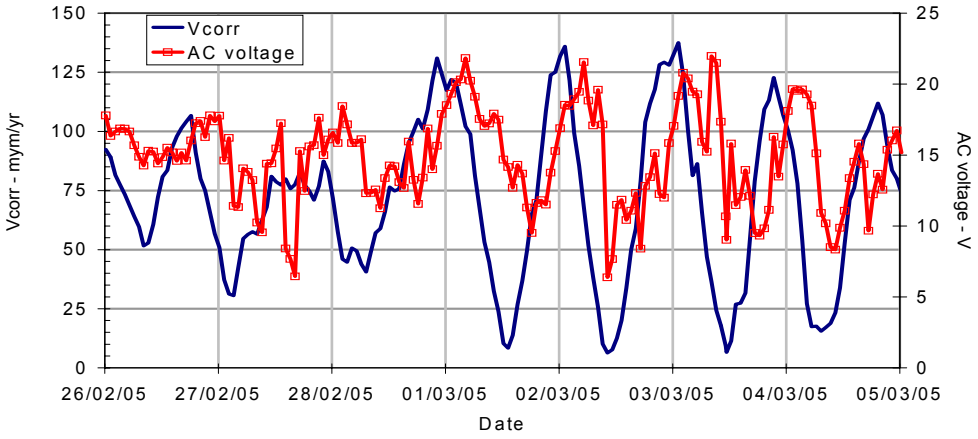

Figure 27. Railway station post– corrosion rate and AC voltage throughout time

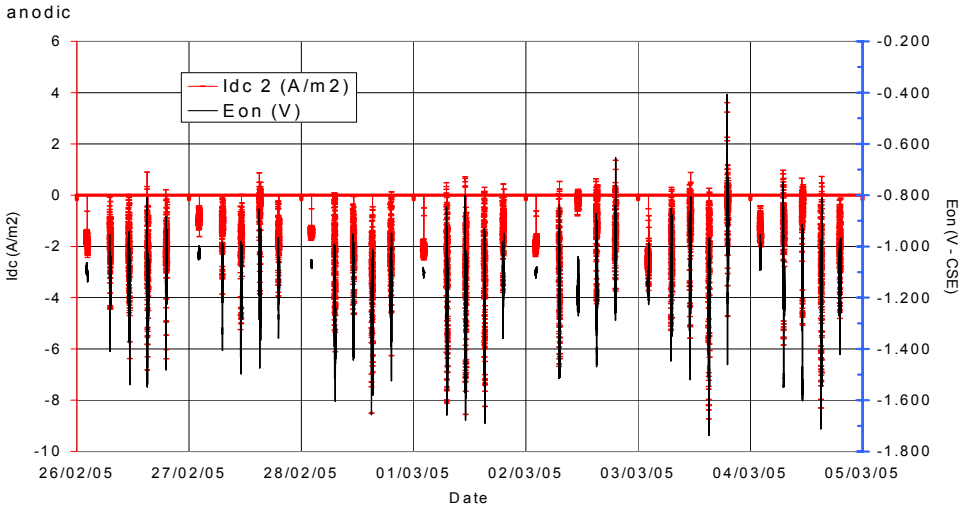

Figure 28. Railway station post – DC stray effect throughout time.

Conclusions - statements

Soil box experiments as well as field research activities have shown that:

1. Cathodic DC density controls the spread resistance at a coating defect.
2. The spread resistance controls the level of AC density – at given AC voltage.
3. High level of DC density (>3-5 A/m2) in combination with (even rather low >5-10 V) AC voltage gives AC corrosion.
4. DC density and spread resistance are primary factors in judgment of AC corrosion likelihood.
5. Combined effect of DC stray currents and AC may cause corrosion both in terms of the alkalisation mechanism that characterises “traditional” AC corrosion, and in terms of the anodic DC peaks occurring in DC stray interference.

Acknowledgements

The financial support by the Danish Gas Technology Centre (DGC) is very highly appreciated.

References

1. L.V. Nielsen, B. Baumgarten and P. Cohn, On site measurements of AC induced corrosion: Effect of AC and DC parameters, Proc. CeoCor 2004, Dresden.
2. CeoCor booklet on AC corrosion, CeoCor 2000.
3. F. Stalder et al., AC corrosion on cathodically protected pipelines, Proc. 5th international congress CeoCor, Brussels, Belgium, CeoCor, 2000.
4. L.V. Nielsen et al, AC induced corrosion in pipelines; detection, characterisation and mitigation, CORROSION ‘2004, Paper No. 04211, 2004
5. L.V. Nielsen, Role of Alkalization in AC induced corrosion and consequences hereof in relation to CP requirements, CORROSION (NACE)‘2005, Paper No. 05188, 2005.
6. L.V. Nielsen, F. Galsgaard, Sensor technology for on-line monitoring of AC induced corrosion along pipelines, CORROSION (NACE) ´2005, Paper No. 05375, 2005.
7. Evaluation of a.c. corrosion likelihood of buried pipelines. Application to cathodically protected pipelines. Draft Corrigendum to EN 12954. CEN TC 219 No 329.